Numerical Investigation of Stresses in Transverse Fillet Weld Lap Joint

By

Muhammad Zeeshan

(Registration No: 00000320427)

Thesis Supervisor: Dr. Hasan Aftab Saeed

Department of Mechanical Engineering

College of Electrical and Mechanical Engineering (CEME)

National University of Sciences and Technology (NUST)

Islamabad, Pakistan

(2023)

THESIS ACCEPTANCE CERTIFICATE

Certified that final copy of MS/MPhil thesis written by Mr. **NS Muhammad Zeeshan**, Registration No. **00000320427** of **NUST College of E&ME** has been vetted by undersigned, found complete in all respects as per NUST Statutes/Regulations, is free of plagiarism, errors, and mistakes and is accepted as partial fulfillment for award of MS/MPhil degree. It is further certified that necessary amendments as pointed out by GEC members of the scholar have also been incorporated in the said thesis.

Signature: _____

Name of Supervisor: **Dr. Hasan Aftab Saeed**

Date: 26-09-2023

Signature (HOD): _____

Name: **Dr. Imran Akhtar**

Date: 26-09-2023

Signature (Dean): _____

Name: **Dr. Nasir Rashid**

Dated: 26-09-23

NUMERICAL INVESTIGATION OF TRANSVERSE FILLET WELD LAP JOINT

By

Muhammad Zeeshan

(00000320427)

A Thesis

Of

Master of Science

Submitted to

Department of Mechanical Engineering

College of Electrical and Mechanical Engineering (CEME)

National University of Sciences and Technology (NUST)

Islamabad, Pakistan

In partial fulfilment of the requirements for the degree of

Master of Science Mechanical Engineering

September 2023

Dedication

Dedicated to my respected parents especially to my beloved late mother whose tremendous support and cooperation throughout my educational career led me to this wonderful accomplishment

ACKNOWLEDGEMENTS

Due praises are given to Allah Almighty, the Creator, and the Sustainer, without whose instruction not a single minute pass. He who has given us forte and blessed us with plenteousness without any measure. There are no words which can do justice to Him. I am empowered to Read and Write only by Him, who has bestowed upon me the knowledge I carry forward.

Whosoever helped me throughout the course of my thesis, whether my parents or any other individual, was Your will, so indeed none be worthy of praise but You. I am profusely thankful to my beloved parents who raised me when I was not capable of walking and continued to support me throughout every department of my life, specially to my late mother in loving memory.

I would also like to express special thanks to my supervisor Dr. Hasan Aftab Saeed for his help throughout my thesis. I would also like to pay special thanks to Dr. Raja Amer Azim for his generous time for useful tips to using ANSYS Workbench. Each time I got stuck in the analysis section; he helped me out with different solutions. Without his help I wouldn't have been able to complete my thesis. I appreciate his patience and guidance throughout the whole thesis.

I would also like to thank Dr. Naveed Akmal Din and Asst Prof Yasser Riaz for being on my thesis guidance and evaluation committee. I am also thankful to them for their support and cooperation. Finally, I would like to express my gratitude to all the individuals who have rendered valuable assistance to my study.

Engr. Muhammad Zeeshan

ABSTRACT

Transverse fillet lap weld joint is designed for tensile strength as one of the plates exerts shear force while the other one exerts tensile force. So, stress prediction is not easy. Stress distribution at the fillet weld with lap joint is predicted without residual stresses previously. Various experimental and analytical approaches are listed in literature review. Stresses at the fillet weld are obtained only at realistic set of boundary conditions. This work includes stress distribution at the weldment using Coupled Field Transient Analysis in ANSYS workbench. Temperature dependent mechanical and thermal properties of structural steel A992 grade 50 at elevated temperatures upto 2000^0C are used for non-linear analysis. Multi-linear isotropic hardening plasticity model is used for non-linear strain hardening response until necking begins. Moving heat is modelled using ACT extension. Structural distortion is the outcome of this heat flux input and residual stresses are generated due to temperature field developed. Stresses at different paths are predicted in the presence of residual stresses. The findings of this study indicate that stresses obtained are significantly higher in the presence of residual stresses and their behaviour are also changed.

Key Words: Transverse fillet lap weld joint, Numerical investigation, stresses, Moving heat source

TABLE OF CONTENTS

LIST OF FIGURES

LIST OF TABLES

LIST OF ABBREVIATIONS

ASTM	American Society for Testing and Materials
ACT	Ansys Application Customization Toolkit
APDL	Ansys Parametric Design Language
TIG	Tungsten Inert Gas welding
HAZ	Heat Affected Zone

CHAPTER 1: INTRODUCTION

1.1 OVERVIEW

The purpose of this section is to give an insight on the background of fillet welding, intent of study and objectives of the research dissertation. An understanding of the fillet weld behaviour in the real world is presented. These details are applicable in this thesis and highlighted different analytical and experimental results already available with the analysis results.

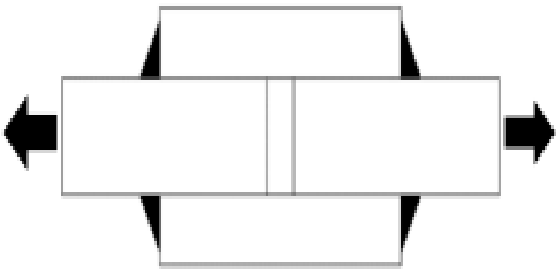

Figure 1-1: Schematic diagram of transverse fillet lap weld joint

1.2 BACKGROUND

Welding is a process of fabrication in which different parts are permanently joined together by the application of high heat to melt parts together and then allowing them to cool. Welding is extensively used in the fields of mechanical engineering, aeronautical engineering, and automotive engineering to assemble parts permanently. Welding includes methods like arc welding and gas welding in which extremely high temperature is generated which melts the parts to be welded. Brazing and soldering are also used for joining parts at relatively low temperatures than in arc and gas welding. Whenever permanent joints with higher strength are required, welding is used. There are different welds, mainly butt weld, fillet weld, lap weld etc. Strength and failure of welded joints depends primarily on type of joints and loading direction.

The most important issue in welded joints is stress calculation at the weld. Sometimes the techniques of strength of materials and of elasticity in the

determination of stress distribution are not successful. Fillet lap weld is obtained by overlapping the plates and then welding its edges. Ther are either longitudinal fillet lap welds or transverse fillet lap welds. Some common fillet welds are illustrated in following figure;

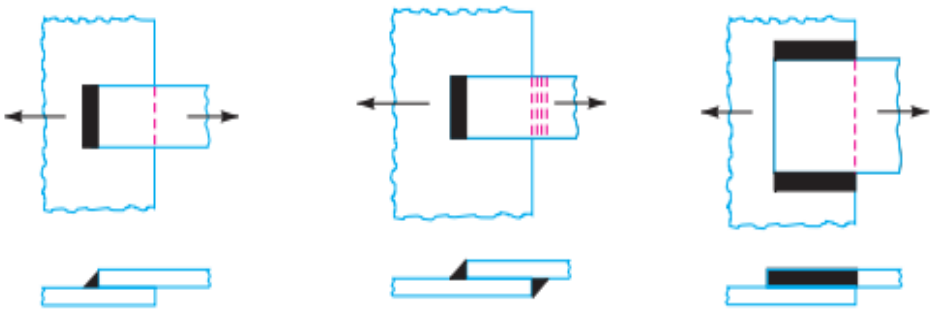

Figure 1-2: Common fillet weld joints

In parallel fillet lap weld joint, both the plates exert shear force on the weld joint while in case of transverse fillet lap weld joint one plate exerts shear force while the other one exerts tensile or compressive force. Transverse fillet lap weld is designed for tensile strength and parallel fillet weld is designed for shear strength. Typical double transverse fillet lap weld joint is shown below: -

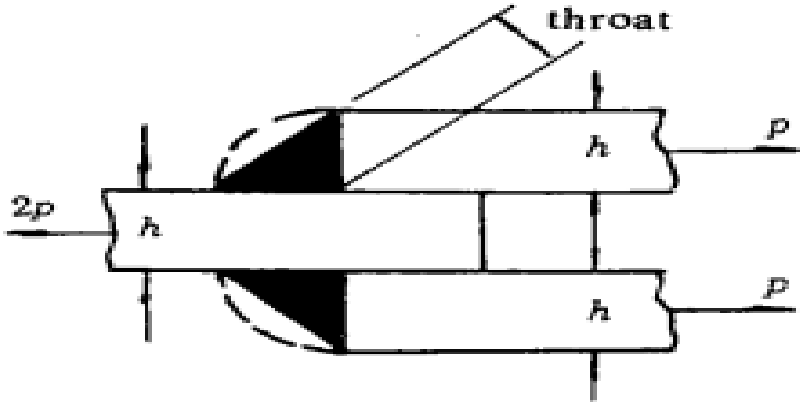

Figure 1-3: Actual configuration of weldment and plates

Since past sixty years, research related to stress distribution in transverse fillet lap welding is still lagging. They only imagine that stress is uniformly distributed

on the fillet welds which is probably wrong and for butt weld it is acceptable that normal stress is uniformly distributed along the weld which is safe to design. The normal and shear stress acting on the fillet throat and using both these stresses for strength control factor cannot be safe and sound.

There are different methods available to calculate stresses in transverse fillet weld lap joint. Different authors and researchers have different approaches to it and there are different results from each technique. Shigley in his book discussed a conventional technique to calculate stress in transverse and longitudinal fillet lap weld joint.

When the fillet weld is parallel to the load applied then weld will fracture in shear while in the case when fillet weld is perpendicular to the load applied then the weld will fracture in tensile.

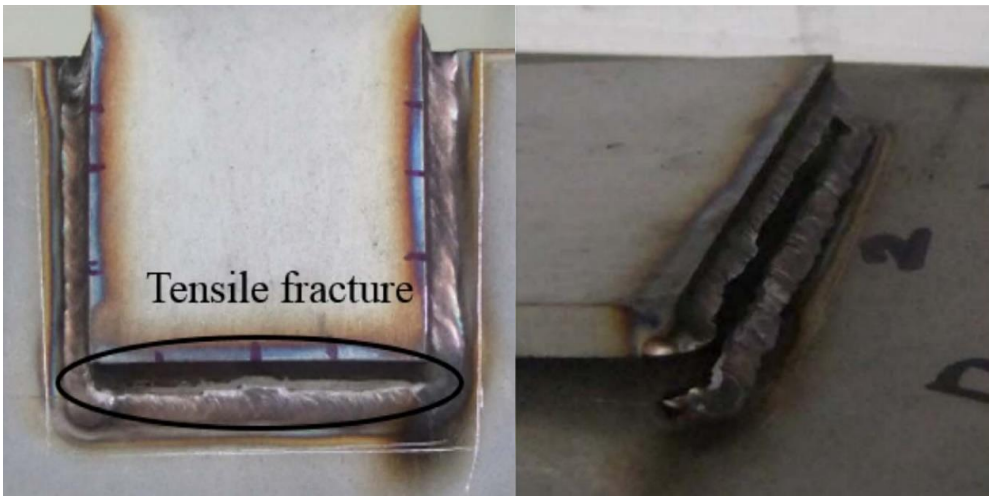

Figure 1-4: Tensile fracture in lap weld joint

In the past, residual stresses were measured experimentally through X-ray diffraction technique and numerically and numerically through different software's. The advantage of numerical methods over experimental methods is the capability of computational techniques in predicting the residual stress state.

1.3 PROBLEM STATEMENT

Fillet welds are extensively used to transmit load from one structural part to another part. A weld may be oriented at any specific direction defined by the angle between weld length and line of action of force. Experiments have revealed that strength of welding depends upon that angle. Stress calculation in the case of butt weld is simple but to calculate maximum stress in transverse fillet weld is not that simple. For butt weld, uniform normal stress distribution is reasonable and safe to design but for transverse fillet weld, uniform distribution of normal and shear stresses is not acceptable and not safe to design. Shear stress in transverse fillet lap welded joint is calculated conventionally in the weakest plane i.e. at the throat section in the weld which has minimum area. As one plate in transverse fillet lap weld exerts shear force while the other one exerts tensile or compressive force. So, it is very difficult to predict normal and shear stresses at the weldment. The aim of this dissertation is to numerically investigate normal and shear stresses at the weldment using realistic boundary conditions to validate our results already listed in literature through experimental and analytical approach. And then we will predict stress distribution and its behaviour in the presence of residual stresses using coupled field transient analysis.

1.4 OBJECTIVES

The research work in this dissertation is presented in two portions. The first portion includes the summarization of different techniques available for determining the stresses in the transverse fillet lap weld joint including conventional method. The second part is related to Finite Element Analysis of transverse fillet lap weld joint with different boundary conditions. The numerical modelling of transverse fillet welded joint is quite challenging. The main objective of this section is to simulate normal and shear stresses at the horizontal, vertical legs of the weld and at the throat section using realistic set of boundary conditions without influence residual stresses. Then we consider the effect of residual stresses by modeling the moving heat source and then calculate these stresses in the presence of residual stress to check how they influence the results.

1.5 THESIS OUTLINE

There are five chapters in this dissertation. A thorough introduction to stresses in transverse weld lap joint is given in the first chapter. Problem statement and research objectives are also included in Chapter 1. A review of the experimental and analytical approaches for stress distribution already existing for transverse fillet lap weld joint is provided in Chapter 2. Also, a review of experimental and numerical approaches already available with residual stresses are discussed in detail in this chapter. Numerical investigation of stresses at the fillet weld in the presence of residual stresses is predicted using coupled field transient analysis by modelling the moving heat source using ACT extension is discussed in Chapter 3. Thorough analysis of the results obtained along with the findings are discussed in Chapter 4. Finally, the conclusions and recommendations for further research are summarized in Chapter 5.

CHAPTER 2: LITERATURE REVIEW

2.1 CONVENTIONAL METHOD

After welding two parts, there are some metallurgical changes taken place in parent metal near the weld region due to heating. Residual stresses are also present there due to the order of welding. If thick plates are to be welded, then pre-heating will be more helpful. For butt welding either in tensile loading or in shear loading, average normal stress is obtained by dividing the force by the weldment area (product of length and throat of the weld) which is quite acceptable and safe to design. Shigley designed the transverse fillet lap weld by using the concept of normal and shear forces acting on the weldment and dividing them individually by throat area will give normal and shear stresses at the throat. Thus, illustrates that maximum shear stress for transverse fillet weld occurs at the throat at 67.5^{o} while maximum von-mises stress occurs at the throat at 62.5^{o}. Thus throat stresses are used for fillet weld design.[1]

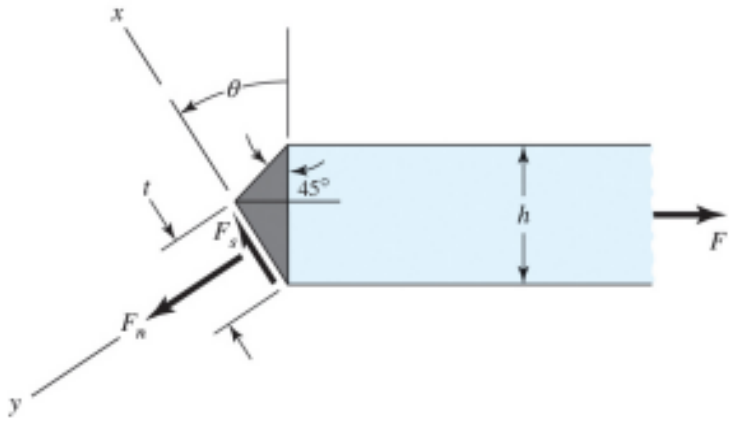

Figure 2-1: Isolated free body diagram of transverse fillet lap weld

Shigley proposed the nominal stresses at angle 'θ' are;

$$\tau = \frac{F_s}{A} = \frac{F\sin\theta}{t\,x\,l} = \frac{F\sin\theta}{\left(\frac{h}{\cos\theta+\sin\theta}\right)l} = \frac{F\sin\theta(\sin\theta+\cos\theta)}{hl} = \frac{F}{hl}(\sin^2\theta+\sin\theta\cos\theta)$$

$$\sigma = \frac{F_n}{A} = \frac{F\cos\theta}{t\,x\,l} = \frac{F\cos\theta}{\left(\frac{h}{\cos\theta+\sin\theta}\right)l} = \frac{F\cos\theta(\sin\theta+\cos\theta)}{hl} = \frac{F}{hl}(\cos\theta\sin\theta+\cos^2\theta)$$

Then, von-mises stress becomes;

$$\sigma' = (\sigma^2 + 3\tau^2)^{\frac{1}{2}} = \frac{F}{hl}[(\cos\theta\sin\theta+\cos^2\theta)^2 + 3(\sin^2\theta+\sin\theta\cos\theta)^2]^{\frac{1}{2}}$$

Shigley proposed von-mises stress to be maximum at $\theta = 62.5^o$ while shear stress to be maximum at $\theta = 67.5^o$ for transverse fillet lap weld joint.

2.2 NORRIS MODEL

In 1945, Norris constructed a model for transverse fillet weld which is used for photoelastic purpose and has the benefit of equal loading situation. Stresses in transverse fillet weld are two dimensional in nature and therefore uniform along the length of weld. In this model, Norris reported the stress distribution at the vertical and horizontal legs of the fillet weld which could be applied to either parent metal or the weld metal. Norris further illustrated that he could only be able to report stress distribution at root and toe of the weld. And he could not be able to find the stresses at the throat of the weld. Several statistical checks applied to the results of Norris model are;

- The resultant normal stress on vertical leg of the fillet weld should be equal to one-half of the tension force applied.
- The resultant shear stress on horizontal leg of the fillet weld should be equal to one-half of the tension force applied.
- The resultant shear stress on the vertical leg of the fillet weld should be equal and opposite to the resultant normal stress on horizontal leg [2].

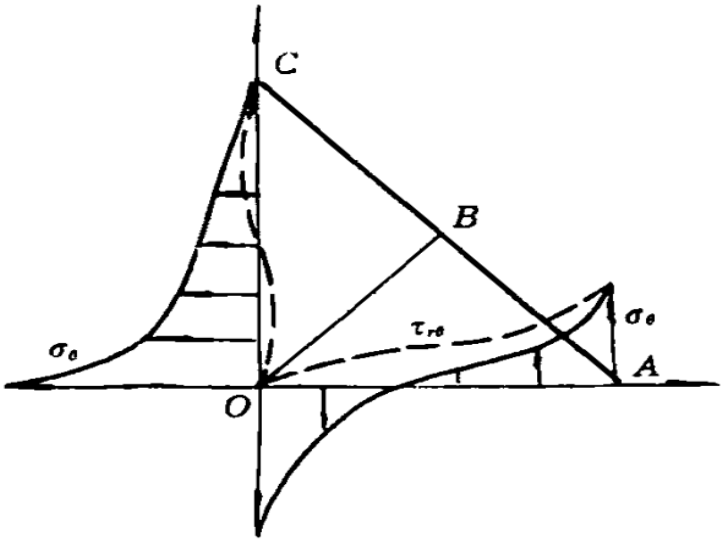

Figure 2-2: Graphical results of Norris Model

2.3 SALAKIAN APPROACH

In 1937, Salakian presents an approach that describes the stresses across the throat section of weld that are used in design. This is applicable only to welding metal and not to parent metal [3]. Maximum principal stress and the maximum shear stress at the root of the fillet weld have same values which is incorrect.

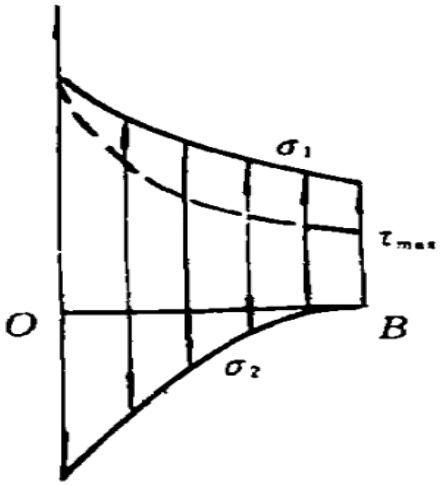

Figure 2-3: Graphical results of Salakian Approach

2.4 NEW SCHEME FOR STRESS CALCULATION

Application of the Theory of Tensional State, Theory of Failure and Thin Wall Profiles Theory are considered to establish new expression of shear stress at throat section of two sheets in lap weld joint which are loaded either transversely or longitudinally. These expressions calculate shear stress without any change to the convention already existent incorporating a coefficient that accounts for the influence of joint dimensions. Thus, eccentricity of load and change in stresses of welds have better approach to have accurate results [4].

$$\tau_{max} = \frac{F}{1.414\ x\ s\ x\ l}\sqrt{\frac{6(s+c)^2}{c} + \frac{2(s+c)}{c} + 0.67}$$

where 's' is the thickness of the sheet while 'c' is the leg of the weld.

$$\therefore k_d = \sqrt{\frac{6(s+c)^2}{c} + \frac{2(s+c)}{c} + 0.67}$$

The term in the bracket is proposed for the modifications of the change in the state tensional due to the eccentricity of load. The vertical leg of the weld must be equal to or less than the thickness of the weld.

2.5 EXACT SOLUTION

In 1995, analytical approach was presented by considering the cross section of seam as quarter of solid circle and by assuming plane problems of theory of elasticity with polar coordinates (r, θ). The equilibrium equations along γ and θ directions are to be satisfied [5]. The relations of all stresses obtained are;

$$\sigma_r = \left(1 - 9\frac{r}{h} + 8\frac{r^2}{h^2}\right)\sigma + 6\frac{\sigma r}{h}\left(1 - \frac{r}{h}\right)sin\theta$$

$$\sigma_\theta = \sigma[1 - 6\frac{r}{h}(3 - 4\frac{r}{h})(1 - sin\theta)]$$

$$\tau_{r\theta} = -6\sigma\frac{r}{h}\left(1 - \frac{r}{h}\right)cos\theta$$

The expression of shear stress indicates that it is zero along the vertical leg of the weld. Normal stress on vertical leg is equal to average stress throughout. The normal stress at the horizontal toe of the fillet weld is seven times the average stress. Also, the graphical representation of these expressions revealed that maximum stress value is not in the throat section of the weld.

The results obtained using analytical formulae of the normal and shear stress is shown below;

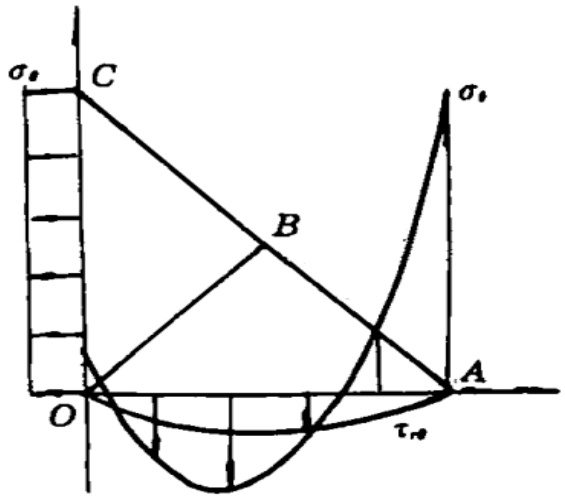

Figure 2-4: Graphical results of normal and shear stress along horizontal and vertical legs

The graphical results of principal and maximum shear stresses at the throat section are shown in fig. 2-5.

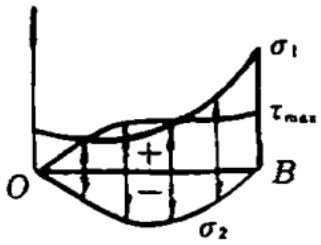

Figure 2-5: Graphical results of principal and maximum shear stress along throat section

2.6 STRUCTURAL-THERMAL ANALYSIS

The analysis of the welded joint is carried out with ANSYS Workbench software [6]. The simulation includes the geometric model created in Design Modeler and fetched in Model where sweep meshing is carried out for all three parts. and analysis is carried out. Then two contacts were defined; one is between two plates and weld and other is between two plates. The contact between plates and weld is defined by critical bonding temperature of 500^0C using commands. As the temperature at the contact surface becomes equal to critical bonding temperature, the contact will become bonded and remain bonded even if temperature becomes lower than critical bonding temperature.

For simulating the thermal field, it is important to model the moving heat source precisely using ACT extension. Moving heat source energy is modeled using Gaussian model. As the moving heat source passes, we get temperature data at different points. To find the stresses due to thermal field generated, temperatures from Thermal analysis are imported into Static Structural at all the calculated steps. Boundary conditions of frictionless support and compression only support is applied, and temperature imported at different steps are the loading conditions. Results of equivalent von-Mises stress and temperature field are obtained.

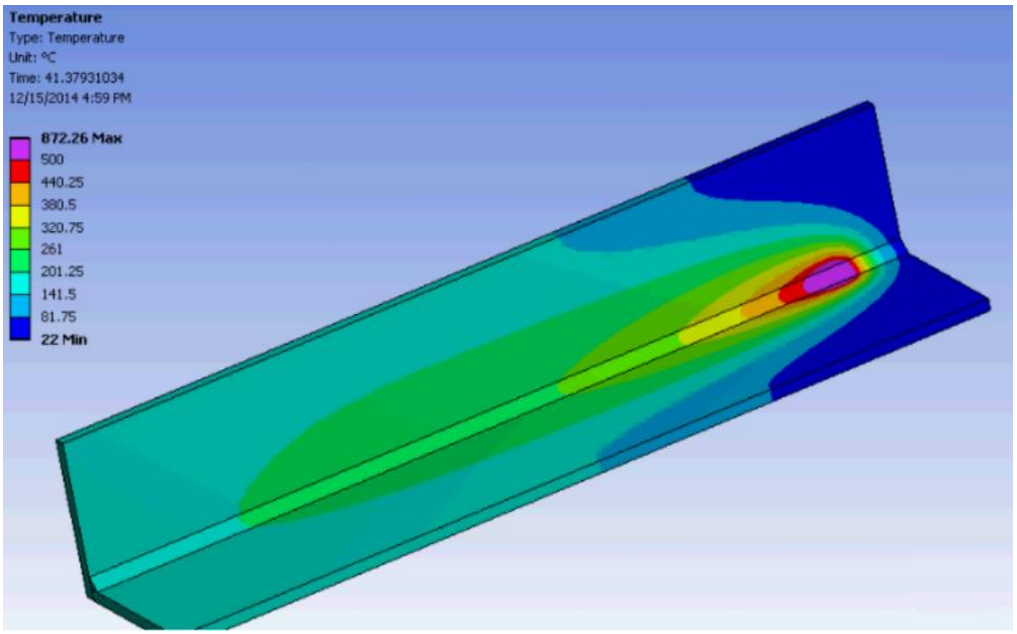

Figure 2-6: Temperature Field

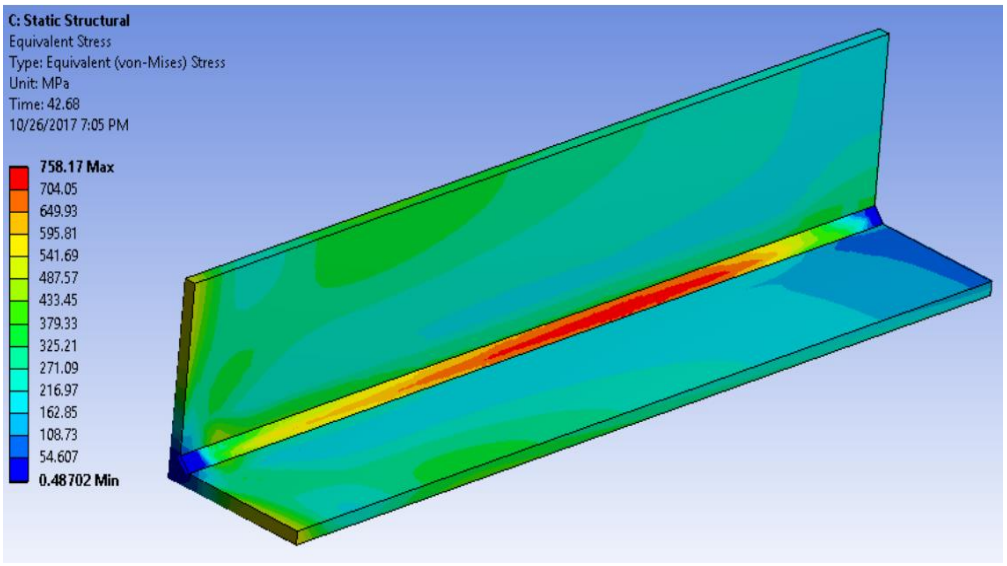

Figure 2-7: Equivalent von-Mises Stress

2.7 SIMPLIFIED FINITE ELEMENT SIMULATION

2D and 3D finite element welding is carried out in this research. T-type fillet weld having plate thickness of 8 mm and 20 mm is simulated using MSC.Marc and ANSYS software's. The sole purpose of this research is to analyze the formation of residual stresses due to the 3D effect of welding process. Residual stresses are measured using X-ray diffraction technique on T-welded structure. Results obtained in 2D simulations are closer to the measured residual stresses. Hence, 2D welding simulation is suggested for predicting residual stresses [7].

The material of weldment and plates are the same i.e., structural steel of grade DH36. The temperature dependent material properties are linearly extrapolated to higher temperatures. Bilinear elastic-plastic model with kinematic hardening is selected. The welding simulation in ANSYS software is carried out sequentially i.e., solving the temperature field in Transient Thermal analysis and then non-linear elastic-plastic deformation. Generalized plane strain formulation of element behavior is used. Moving heat source is passed to simulate temperature field. Following two variations are used for the welding simulation:

- Assuming solid modeling of complete welded structure (solid model)
- Assuming gap at the unfused weld root between plates (contact model)

Residual stresses measured with X-ray diffraction technique and with different software's are;

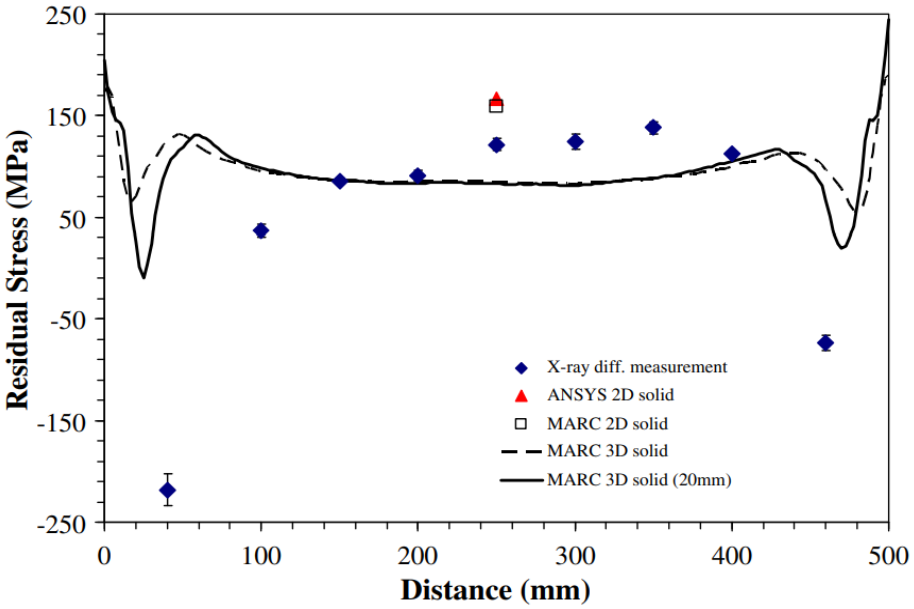

Figure 2-8: Residual stress comparison with solid models

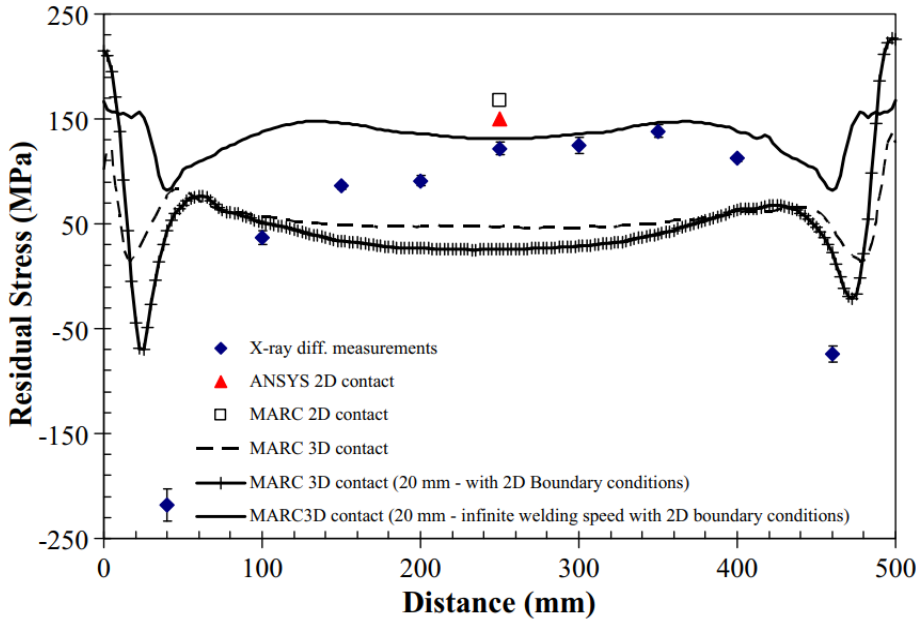

Figure 2-9: Residual stress comparison with contact models

2.8 TEMPERATURE AND RESIDUAL STRESS ANALYSIS

For welding analysis, a physically appropriate heat flux simulation is modelled accurately. Material properties at higher temperature are utilized for the modelling of temperature and residual stresses. The cylindrical moving heat flux model is applied using heat source with constant applied condition. Heat flux mechanism is developed for TIG welding onto stainless steel SS304 material by utilizing temperature dependent thermal properties. Normal conduction, convection and radiation boundary conditions are applied. Boundary conditions applied are summed up as follows.

$$K_n - q + h(T - T_0) + \sigma . \in \left(T^4 - {T_0}^4\right) = 0$$

For thermal analysis, load steps are increased to 1000 seconds after the welding process is complete so that plate cools down and temperature becomes equal to ambient temperature. SOLID70 element type is used for thermal analysis of single pass butt welding. Due to temperature gradient, material properties of stainless steel SS304 were added at elevated temperatures.

Results obtained for temperature distribution and residual stresses are,

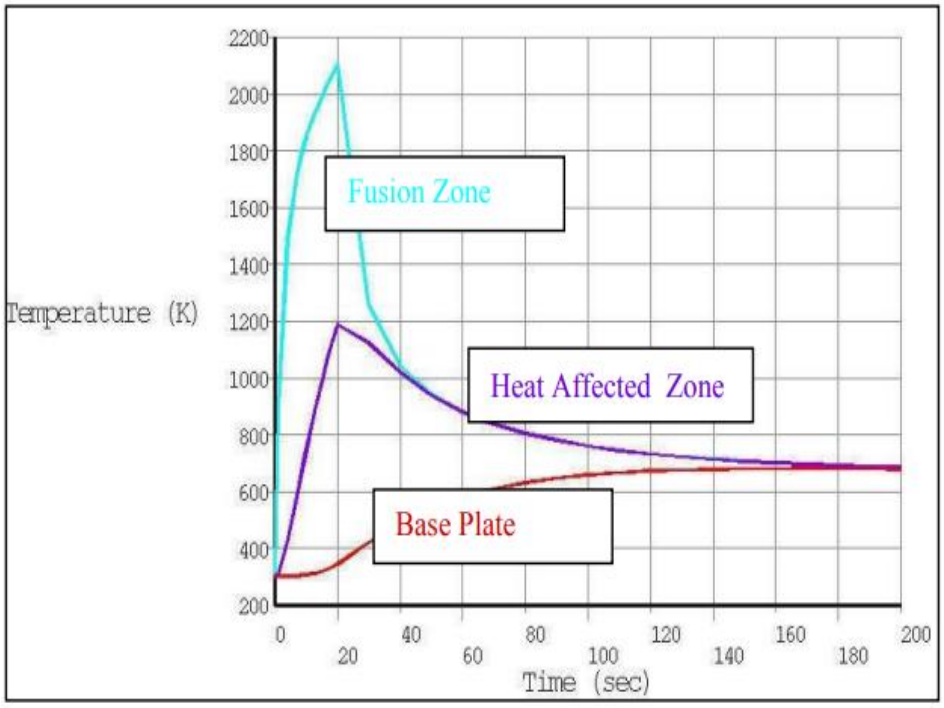

Figure 2-10: Temperature field perpendicular to welding direction at 15s

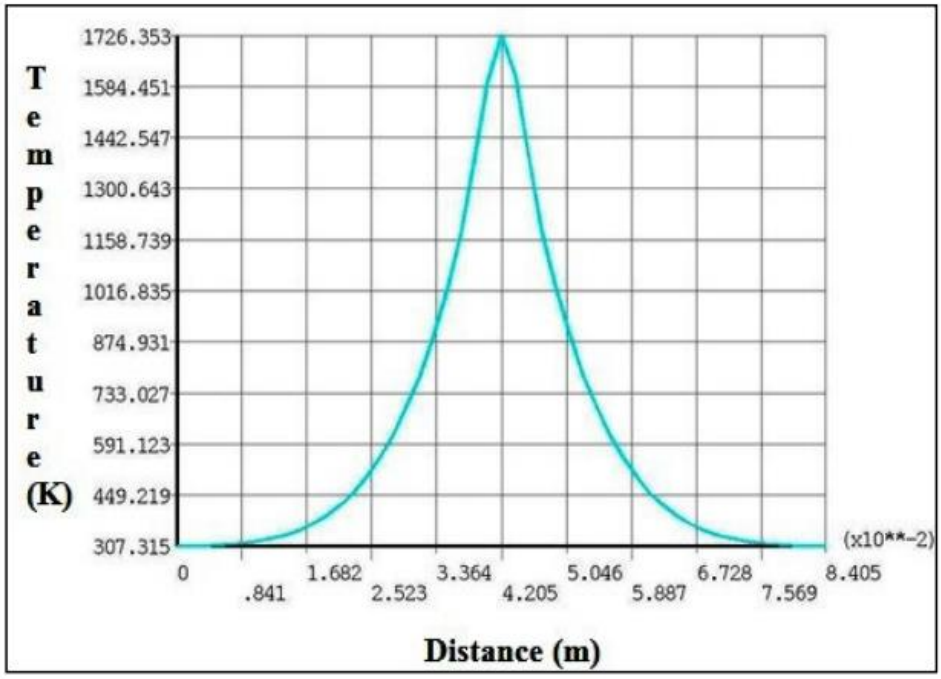

Figure 2-11: Temperature distribution in transverse direction

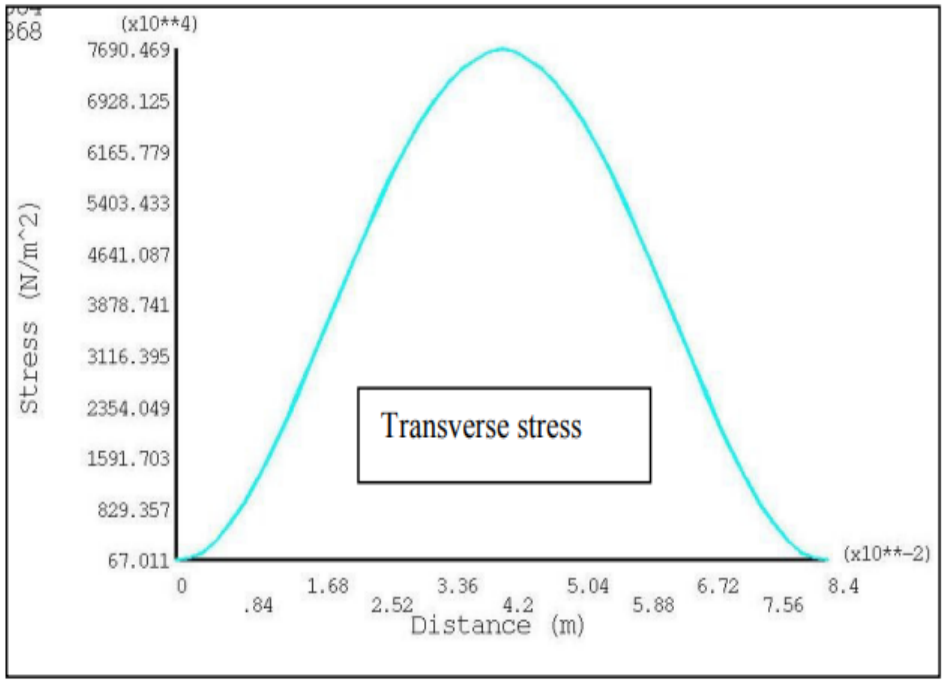

Figure 2-12: Stress distribution in horizontal direction

Transverse stress distribution indicates that the stress is higher in the weldment region and decreases from center line towards the end of the plates. The temperature at the welded region is high as compared to the temperatures at heat affected zone and the base plate region. As distance from heat source is increased the temperature rapidly changes. Higher residual stresses at fusion region are predicted as compared to HAZ and base plate.

CHAPTER 3: METHODOLOGY

The first step is the selection of plates and weldment geometry. Stresses at the weld joint in horizontal, vertical legs and at throat section are simulated using ANSYS software. The simulation is performed using different thickness of plates, size of HAZ to study their effects. Different boundary conditions are applied to validate our results with the results given in literature. The material of plates and welding joints are structural steel. The effect of varying plate thickness, and HAZ on the results is studied using the model generated.

3.1 FINITE ELEMENT MODELING

This section studies geometric modelling, methodology of mesh development and model set-up of transverse fillet lap weld joint.

3.1.1 Modelling

Modelling in finite element method is the critical part of numerical analysis. The whole model is divided into three different parts namely base material, heat affected zone and weld material. The reason for doing so is that we can change the material of any part if we require. The solid model of two plates with lap joint shown in fig. 3-1 is generated using pre-processor of finite element package ANSYS Workbench. Two plates with length of upper plate = 20 mm and length of lower plate = 22 mm are joined together through a fillet weld lap joint. The thickness of both plates is equal to 5 mm. Fillet lap welds have uniform horizontal and vertical leg lengths 5 mm equal to the thickness of the plates. The vertical leg of the weld must be less than or equal to the thickness of the plate, but it must not be greater. The width of the plates and fillet weld is kept 20 mm (extruded in z-direction). Material of plates and weld is same i.e., structural steel. Dimensions of HAZ on both horizontal and vertical legs are 2 x 5 mm each. The geometry of the specimen is shown in fig. 3-1.

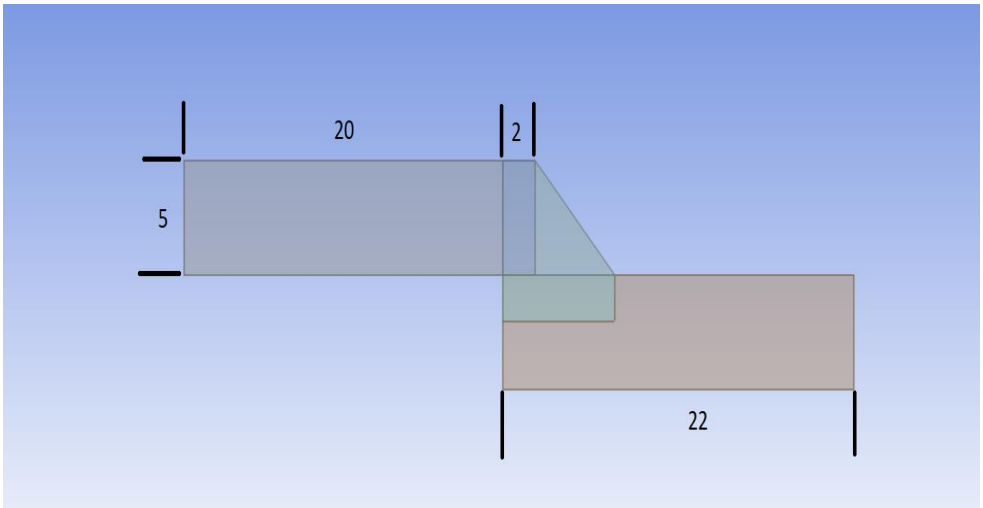

Figure 3-1: Typical geometry of transverse fillet lap weld joint, dimensions in mm

In this model, base metal and welded metal are different parts and in between them there is HAZ. The connected area is the welded material only. As we can see in the connection tab from the model tree, there is only bonded contact between two plates and weld metal through heat affected zone.

3.1.2 Elements and Meshing

The element types used to mesh this model are a 3D quadrilateral element with mesh size of 0.5 mm for both plates and 0.25 mm for the HAZ and fillet weld. The mesh size for the HAZ and weld joint are kept half of the mesh size of plates to assign gradual change in material properties from weld metal to base metal. The final mesh of the model is shown in fig. 3-2. It consists of 360095 nodes and 79840 elements.

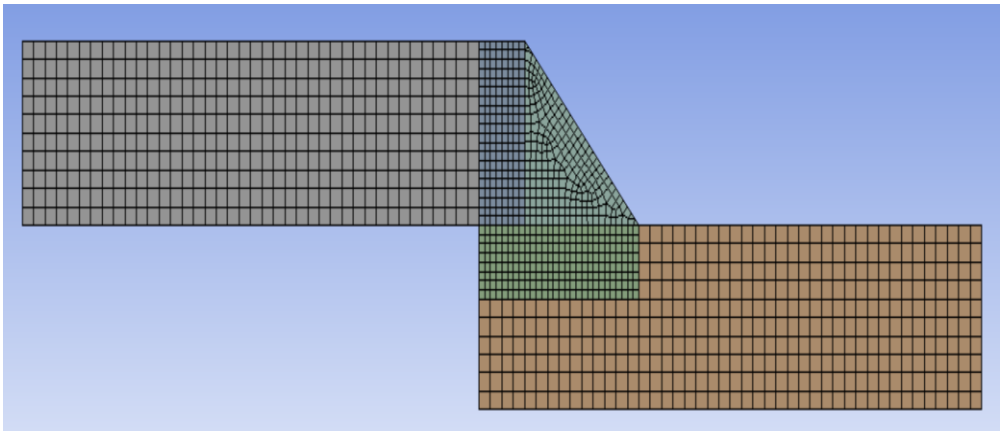

Figure 3-2: Mesh map of Model

3.1.3 Model Set-Up

There are different parameters that are been set-up for this model. The model tree of the model set-up is shown in Fig. 3-3

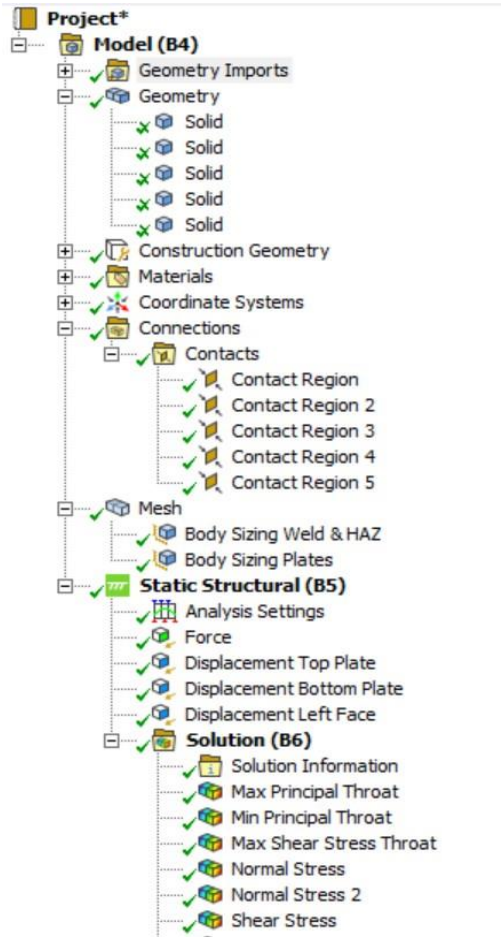

Figure 3-3: Model set-up tree

There are five parts in model including two plates, two heat affected zones and weldment. All have the same material properties i.e., of structural steel. In the mesh set-up, plates and other parts have different element sizes. Plates have element size two times of the element size of HAZ and weldment to have correct stress flow from plate through weldment to the other plate.

3.2 FINITE ELEMENT SIMULATION

Finite element analysis is the practical approach of finite element method, which is mostly used by engineers to numerically solve complex problems. A finite element model consists of a system of points commonly known as nodes which constitutes the design model. Finite elements are connected to these nodes which forms the mesh and have the material and structural properties of model, which defines how to react when certain conditions are applied. The finite element mesh density may vary depending upon the stress level at a certain area. Regions that undergo higher changes in stress level require a higher mesh density than those that undergo a very small or no stress changes.

Finite element models can be developed using one-dimensional, two-dimensional and three-dimensional elements. By using 1D or 2D elements we can create a representative model having less nodes with same accuracy. The general procedure of FEA that shows how it works is shown in Fig. 3-4.

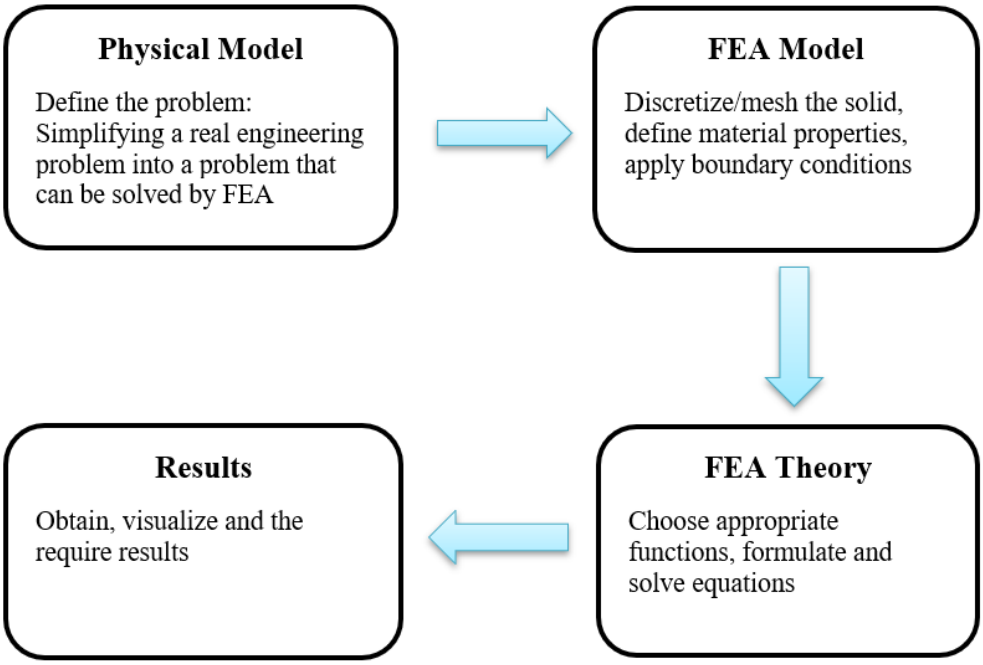

Figure 3-4: General procedure of finite element analysis

3.2.1 ANSYS Simulation

Simulation details of transverse fillet lap weld joint is done with ANSYS 2022 R1. Further simulation details are tabulated in table 3-1.

Table 3-1: Simulation Details

Project Name	Finite element analysis of transverse fillet lap weld joint
FEA tools and version	ANSYS 2022 R1
Analysis Type	Static structural
Material	Structural steel
Unit System	Metric (mm, kg, N, mV, mA)
Force Applied	100 N
Connections	Total 5 bonded connections
Mesh	Mesh with element size of 0.5 mm for plates while 0.25 mm for weldment.
Nodes	360095
Elements	79840

3.2.2 Boundary conditions and loading

To simulate, the left face of the top plate is constraint in x-direction while on right side of the bottom plate, tension force of 100 N is applied. All faces of both the top and the bottom plates excluding already loaded and constraint faces are constraint in y and z-directions to validate our results with results listed in literature review.

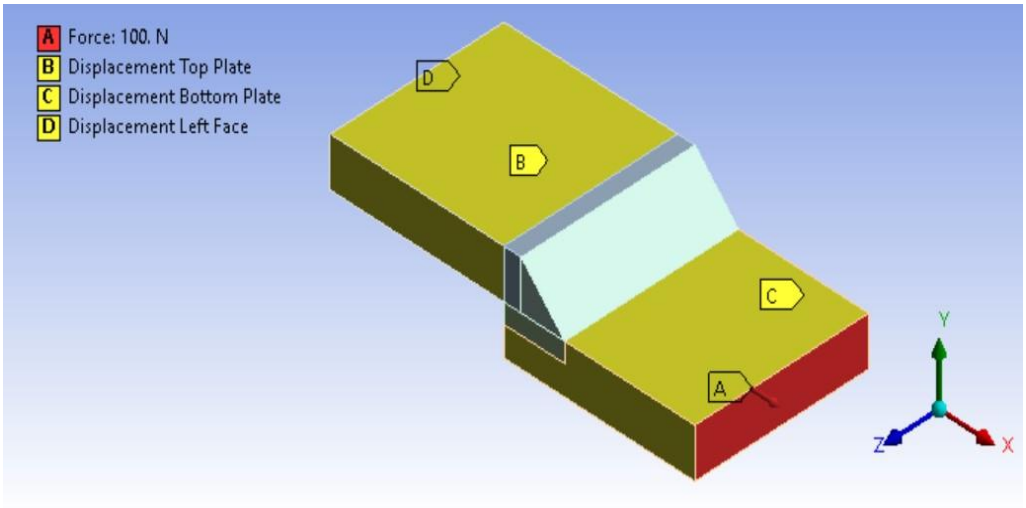

Figure 3-5: Model with constraints and load applied

3.2.3 Effect of Plate Thickness

The thickness of the plate is varied to study its effect on stress distribution in throat section of the weldment. Loading and boundary conditions are the same during the variation in plate thickness. As we increase the thickness of the plate, stress values decrease but the trend of the stress distribution remains the same.

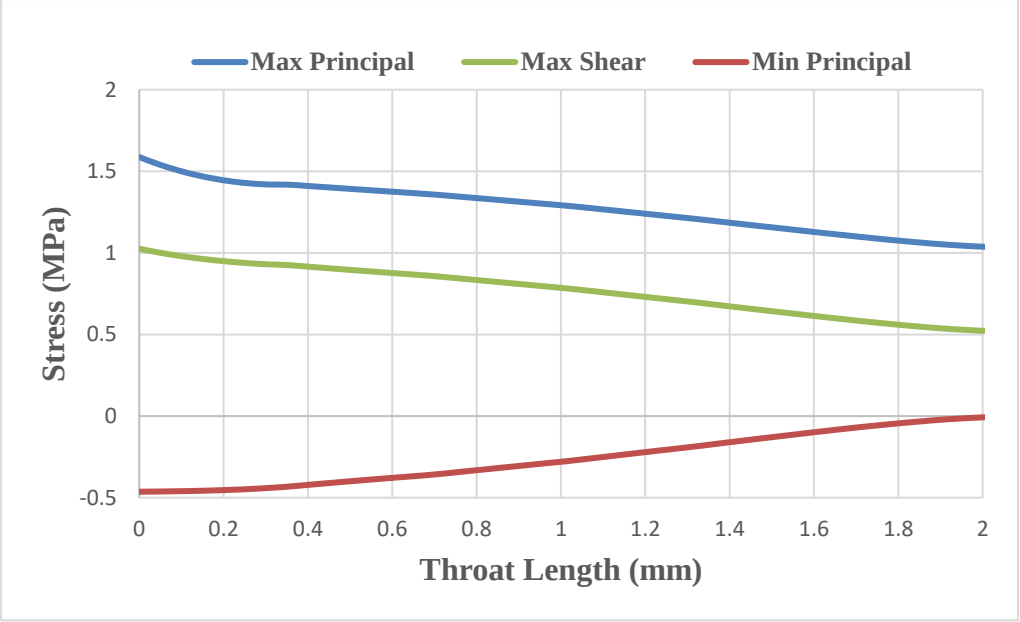

Figure 3-6: Maximum shear and principal stress distribution at throat with 3 mm plate thickness

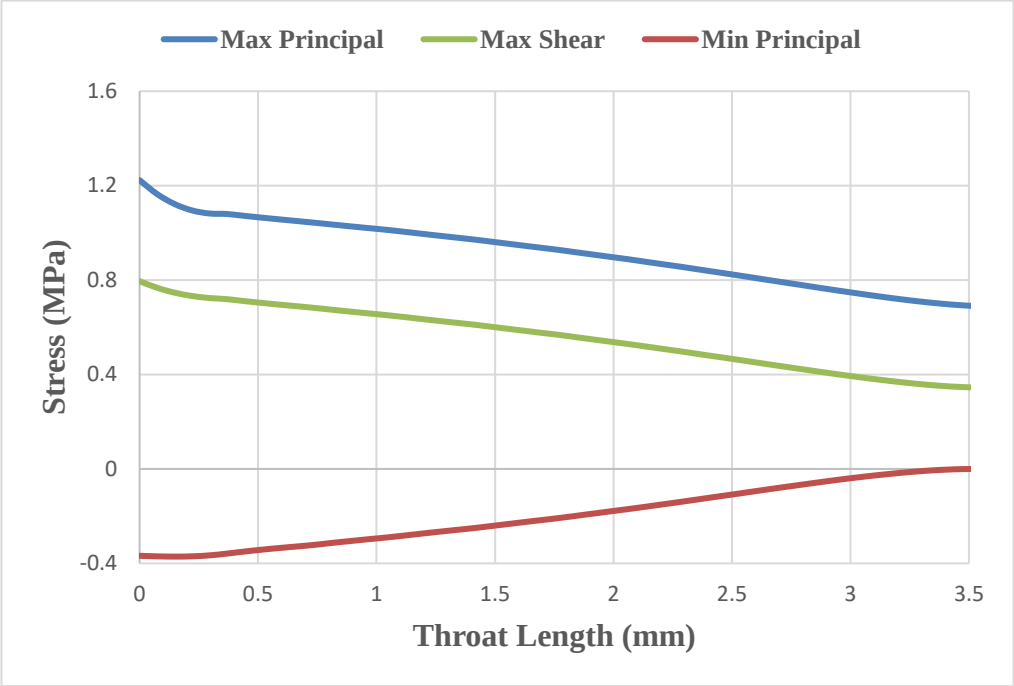

Figure 3-7: Maximum shear and principal stress distribution at throat with 5 mm plate thickness

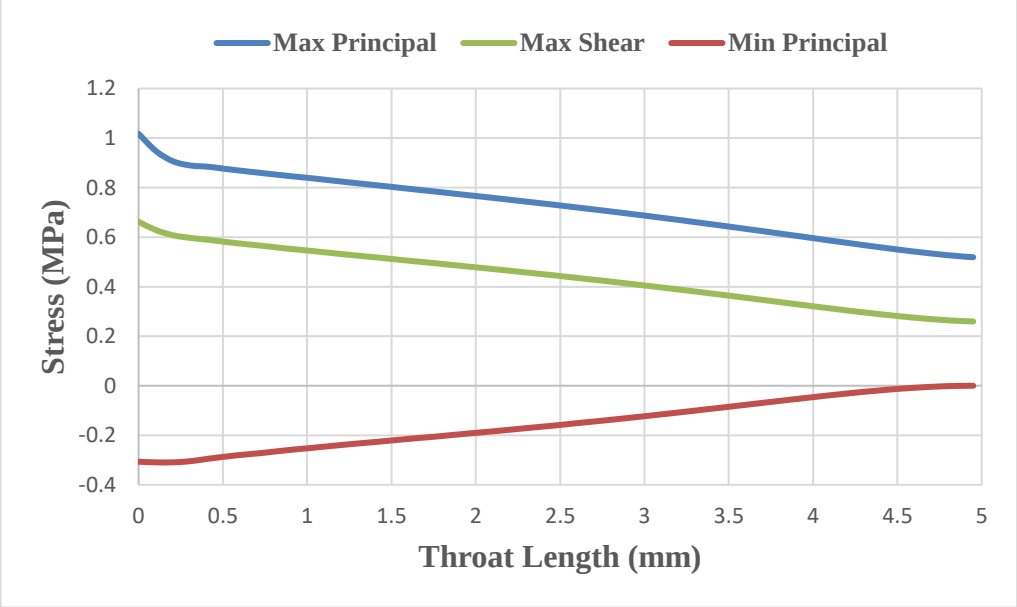

Figure 3-8: Maximum shear and principal stress distribution at throat with 7 mm plate thickness

3.2.4 Effect of Heat Affected Zone

Heat affected zone area is varied to study its influence on the stress distribution in throat section of the weldment. The thickness of the plate is kept constant i.e., 5mm and other constraints and loading conditions are same. HAZ with 1mm and 3mm dimensions are discussed and plotted below;

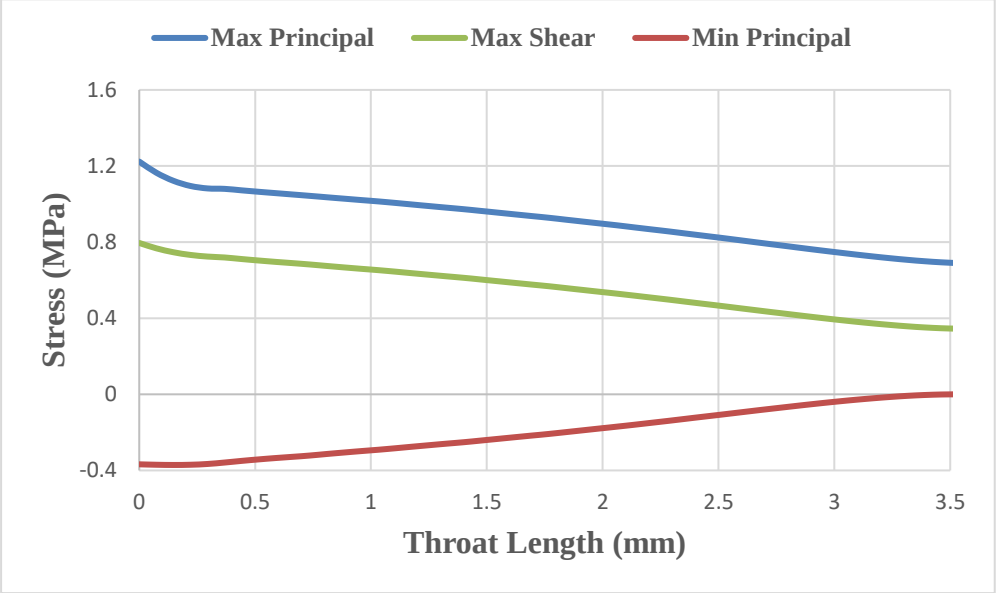

Figure 3-9: Maximum shear and principal stress distribution at throat with HAZ 1 mm

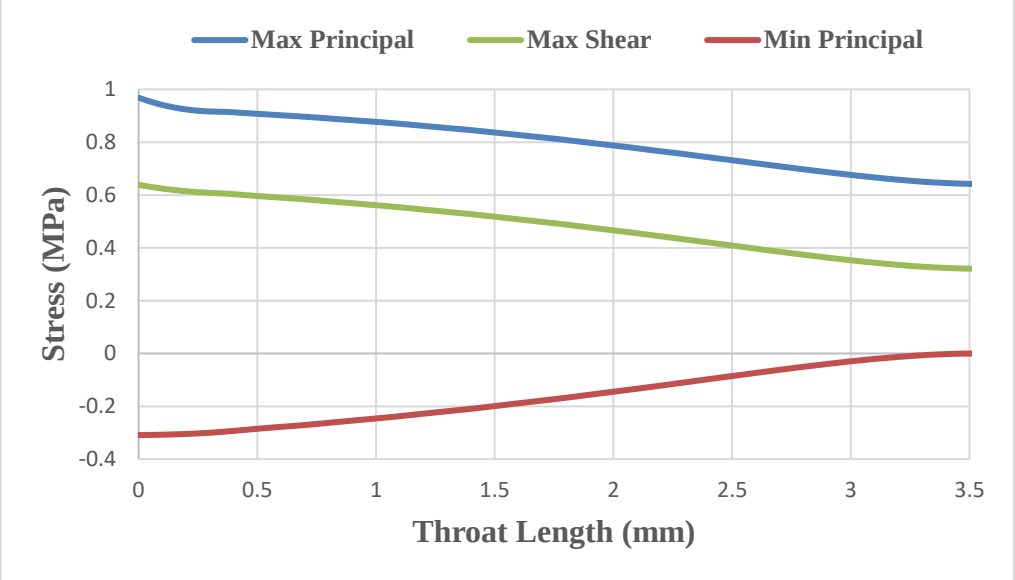

Figure 3-10: Maximum shear and principal stress distribution at throat with HAZ 3 mm

As the heat affected zone increases, the stress values approach zero but the trend of stress distribution remains the same.

3.3 COUPLED FIELD TRANSIENT ANALYSIS

Previously, we have simulated the design weldment with different constraints to validate our simulation results. But now we will also consider the residual stresses which are the stress fields that occur in the absence of external loads. For this purpose, we will create an elasto-plastic model in Coupled Field Transient to simultaneously apply thermal and structural analysis. Also, we will select Structural Steel NL from general non-linear materials in Engineering Data Sources. Under isotropic elasticity, we will add Youngs Modulus and poison ratio values at elevated temperatures with more data points.

Yield stress does not take part in analysis, but it can have its influence on the stiffness of material in case of non-linear analysis. For non-linear analysis, we specify material properties as a function of temperature i.e., adding material properties at different temperatures. So, we will also add thermal properties of material like thermal conductivity, specific heat and coefficient of thermal expansion at different temperatures.

The thermal and mechanical properties of structural steel grade A992 grade 50 at different temperatures are illustrated in table 3-2 as given by [7,9].

Table 3-2: Temperature Dependent Thermal and Mechanical Properties of Structural Steel A992 grade 50

Temperature (°C)	**Elastic Modulus (MPa)**	**Poisson Ratio**	**Thermal Expansion Coefficient 10^{-5} (1/°C)**	**Thermal Conductivity (W/mmC)**	**Specific Heat (J/Kg°C)**
20	205000	0.27	1.17	53.4	439
200	196000	0.29	1.2	48.4	530
400	171000	0.32	1.32	43.5	606
600	122000	0.35	1.39	39	760
800	56000	0.37	1.45	33.5	803
1000	10000	0.39	1.52	26.5	688
1200	1500	0.42	1.59	21	684
1400	1000	0.44	1.65	27	790
1600	80	0.46	1.71	102	681
1800	0.1	0.48	1.77	198	800
2000	0	0.49	1.82	300	800

We can define strain hardening portion in Ansys Workbench by using either bilinear isotropic hardening or by multilinear isotropic hardening.

A bilinear isotropic hardening assumes linear strain hardening portion and is defined using tangent stiffness which is the slope of this straight line whereas multilinear isotropic hardening uses a piece-wise linear function to model the non-linear strain hardening response until necking begins. Comparison between different elasto-plastic models is visualized in fig. 3-11. Multilinear strain hardening is closer to the real stress strain curve, so we get more accurate results by using multilinear strain hardening instead of bilinear strain hardening.

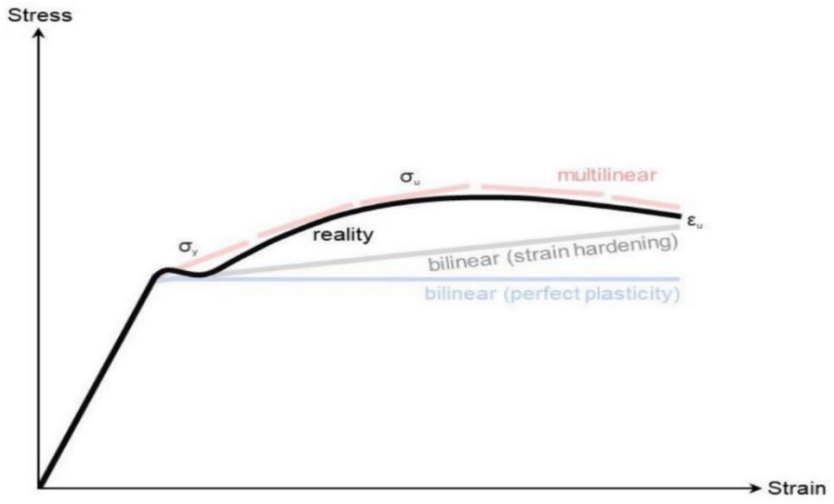

Figure 3-11: Comparison of different elasto-plastic models

As in multilinear isotropic hardening, plastic behaviour is closer to reality than bilinear isotropic hardening, so we use this one. So, we will input the data values of stress against plastic strain calculated from stress strain curve at elevated temperatures.

True stress-strain values are obtained from engineering stress strain curve from the following relations;

$$\sigma_{true} = \sigma_{eng} \times (1+\varepsilon_{eng})$$

$$\varepsilon_{true} = \ln (1+\varepsilon_{eng})$$

The true stress-strain curve for ASTM A992 with 5% true strain at elevated temperatures is shown in fig. 3-12.

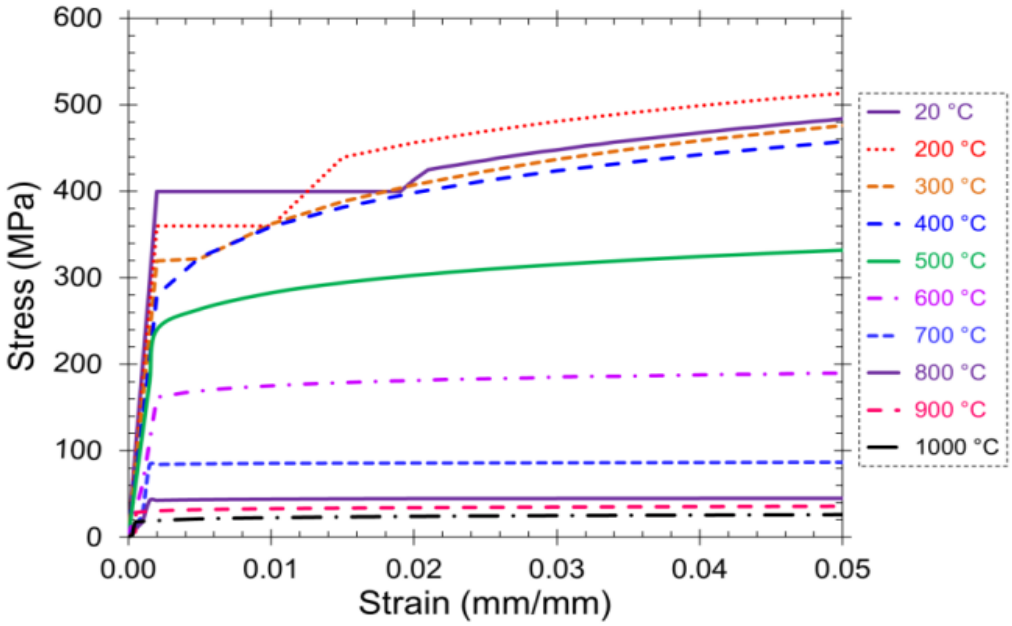

Figure 3-12: True stress-strain curves for ASTM A992 [41]

We have calculated plastic strain values from total true strains as;

$$\varepsilon_{plastic} = \varepsilon_{total} - \varepsilon_{elastic}$$

$$\therefore \varepsilon_{elastic} = \frac{\sigma_{\text{true}}}{E}$$

The first data point must be yielding stress at zero plastic strain. We have interpreted plastic strain values from graph for each true stress value at elevated temperatures.

3.3.1 Model Development in Coupled Field Transient Analysis

Two overlapping plates with fillet weld are modelled in Design Modeler and then it is brought in Mechanical application for meshing and analysis. Plate dimensions are increased to (150 x 100) mm to overcome convergence issues. Sweep mesh is used for all the parts in geometry. Lower order elements were used for meshing. Frictionless contact is created between the plates and bonding contact is defined between the plates and the weldment.

3.3.2 Moving Heat Source

To simulate thermal fields in welding, moving heat source is modeled using ACT extension available in ANSYS Workbench. SOLID226 element type is used. Loading conditions for moving heat flux are;

- Moving Heat Flux: Velocity of source = 12.5 mm/sec; Source power intensity= 1040 W/mm^2; Start time = 0 sec; End time = 8 sec; Radius of Beam = 4 mm
- Convection: Film coefficient (0.0001 W/mm^{2}C)

A Gaussian model is used to define a moving heat source energy which has following equation;

$$E = Ae^{-\frac{[(x-x_o)^2+((y-y_o)^2)]}{B^2}} . e^{-\alpha(z-z_o)}$$

where,

E = Heat Energy

A= Radius of the beam

B= Source Power Intensity

α = Absorption Coefficient

(x_0, y_0, z_0) = Instantaneous position of the center of the heat flux on the path

v = Speed of the moving heat source

t = Time (x_0, y_0, z_0)

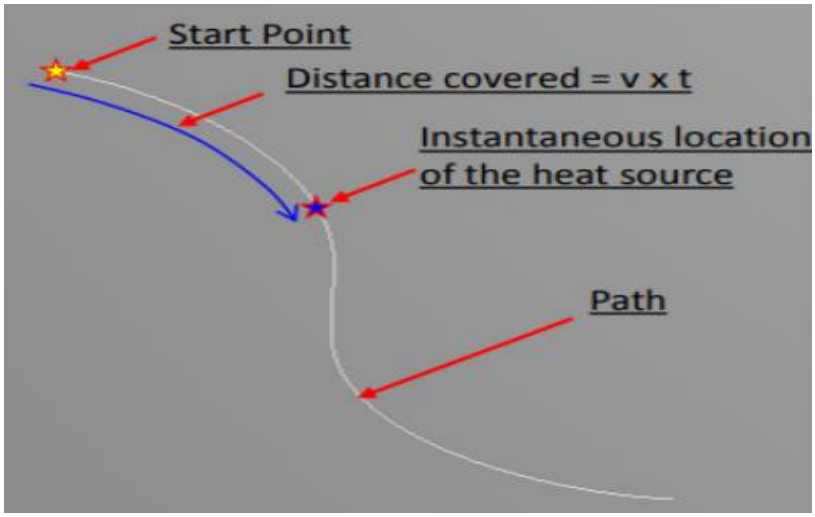

Figure 3-13: Moving heat source

Thermal and structural loads in coupled field transient analysis are applied in different loadsteps. Both far ends of the plates are constraint during the complete simulation. During the first loadstep heat source is moved over the fillet weld for the first 10 seconds. After the heat source is moved then we give 240 seconds as cooling time so that temperature drops below than 100^0C. So residual stresses are produced as result of temperature field generated. Then we apply x-component of tension force of 100 N on the right face of the bottom plate. Now we will get the results of temperature field and required structural stresses at the fillet weld.

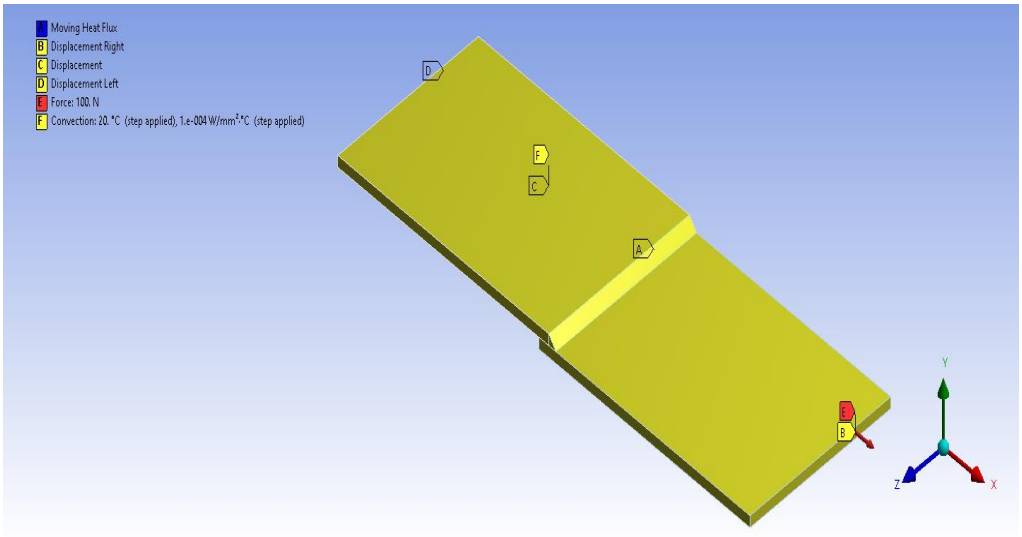

Figure 3-14: Thermal and structural loads for coupled field transient analysis

Boundary conditions applied are;

A. Moving heat flux is applied on the fillet weld.
B. The bottom faces of both plates are constraint in y-axis.
C. The right side of the bottom plate is constraint in y-axis.
D. The left face of the top plate is constraint in all axes.
E. The X-component of tension force 100 N is applied on the right side of the bottom plate after cooling.
F. Convection is applied on all the exposed surfaces.

CHAPTER 4: RESULTS AND DISCUSSION

We have obtained different results from different methods. Each result is discussed below;

4.1 SHIGLEY CONVENTIONAL METHOD

Nominal stresses at angle 'θ' in the weldment are;

$$\tau = \frac{F}{hl}(sin^2\theta + sin\theta cos\theta)$$

$$\sigma = \frac{F}{hl}(cos\theta sin\theta + cos^2\theta)$$

As in our problem, tension force applied is 100 N, weld leg size is 5 mm and length of weld is 20 mm.

For $\theta=0^0$, horizontal leg $\tau = 0$, $\sigma = 1$ MPa

For $\theta=90^0$, vertical leg $\tau = 1$ MPa, $\sigma = 0$

For $\theta=45^0$, throat section $\tau = 1$ MPa, $\sigma = 1$ MPa

As Shigley design the fillet weld on throat section for safety, so shear and normal stresses would be 1 MPa.

4.2 STRESS DISTRIBUTION WITHOUT RESIDUAL STRESSES

Stress distribution at the fillet weld along the vertical, horizontal legs and throat section is simulated with plate thickness of 5 mm and HAZ of 2 mm. Boundary conditions applied are the left face of the top plate is constraint in x- axis, so that it can't move in horizontal direction. Both the plates are constraint in y and z axis and tension force of 100 N is applied in x-component. We get the stress distribution validated with Salakian Approach mentioned in literature review.

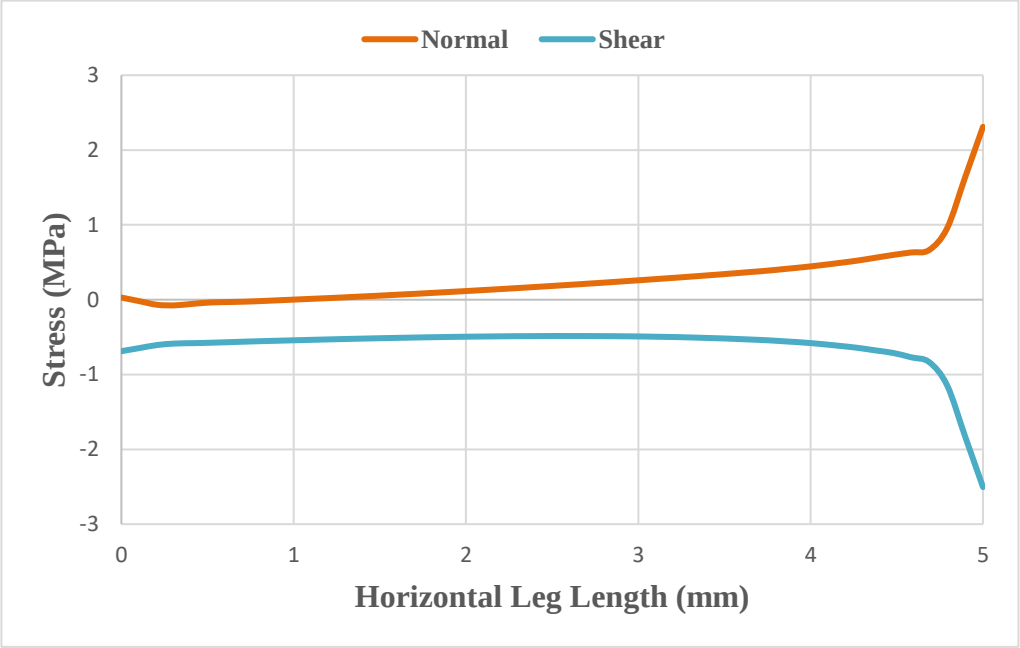

Figure 4-1: Stress distribution along horizontal leg

Stress distribution at the horizontal leg shows clearly sudden increase in the normal stress and sudden decrease in shear stress just near the horizontal toe. Also stress concentration occurs at the horizontal toe of the fillet weld.

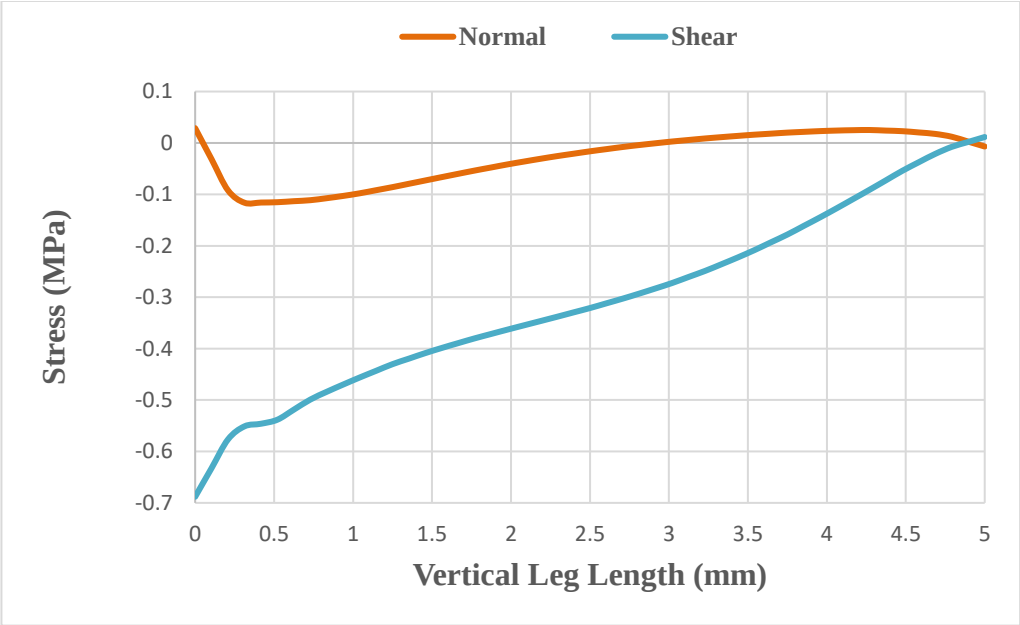

Figure 4-2: Stress distribution along vertical leg

Stress distribution at the vertical leg of the fillet weld indicates almost zero stresses at the vertical toe and gradually increases till the root of the fillet weld.

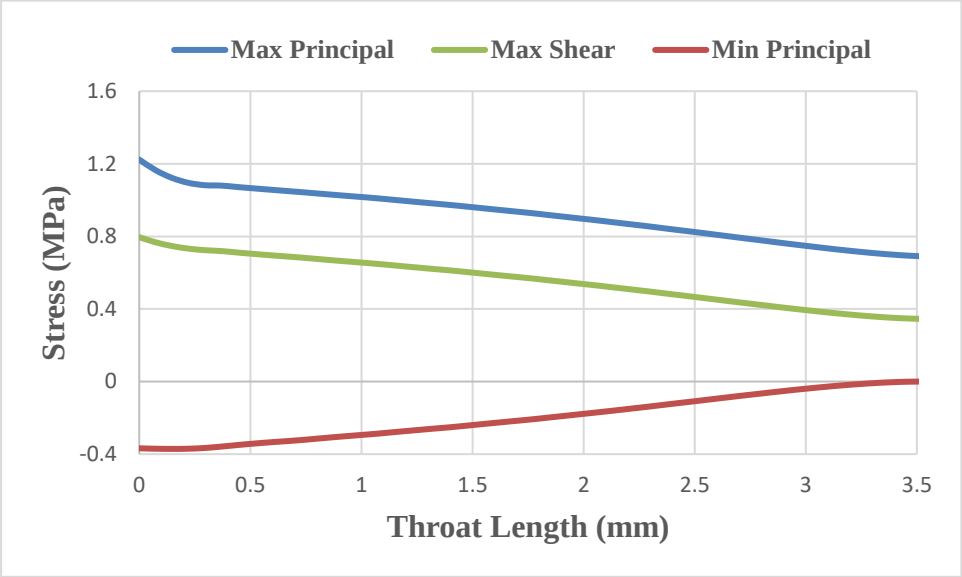

Figure 4-3: Stress distribution along throat length

Stress distribution at the throat section indicates the stress concentration at the root of the fillet weld and then it gradually decreases towards the throat with minimum principal stress approaching almost zero value.

4.3 STRESS DISTRIBUTION WITH RESIDUAL STRESSES

When we modeled the problem using Coupled Field Transient Analysis then residual stresses have impact on stress distribution. Stress becomes quite high due to the residual stresses generated in the model.

Plastic strains at the starting are lower because temperature is not distributed in the starting. As the heat source moves on, plastic strains increase.

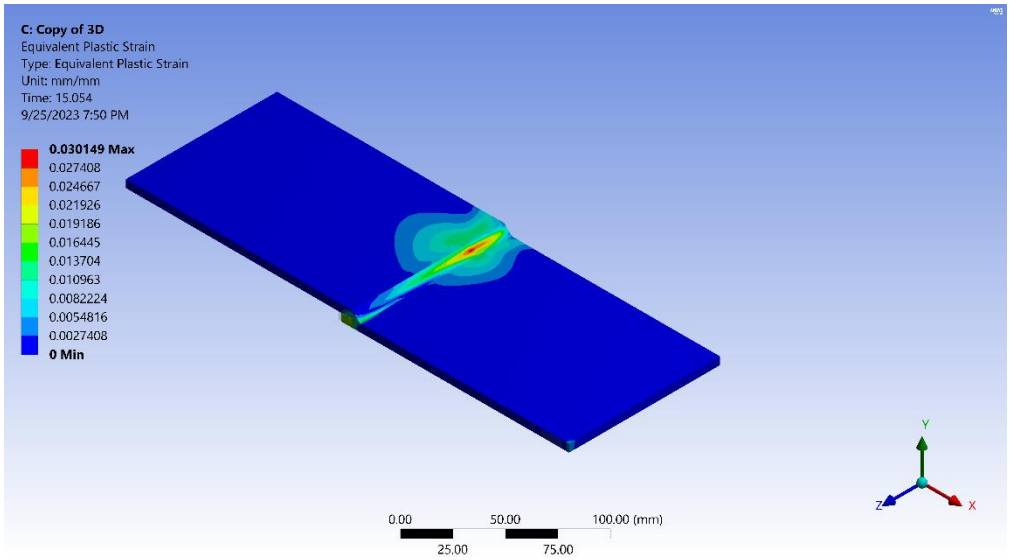

Figure 4-4: Equivalent plastic strains

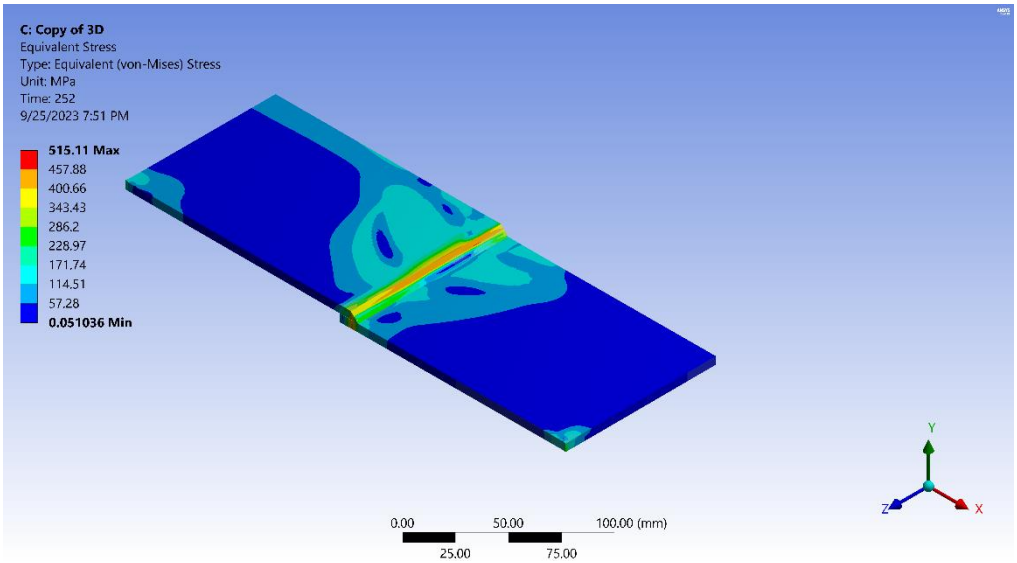

Figure 4-5: Equivalent Stress

The temperature versus time graph indicates that as the heat source is moved over the weldment surface, the temperature gradually increases from initial 22^0 to above 1800^0 due to conduction. The temperature at the weld region is found to be higher than any other area. At time t = 8 sec, highest temperature is achieved, and it gradually drops thereafter due to convection applied.

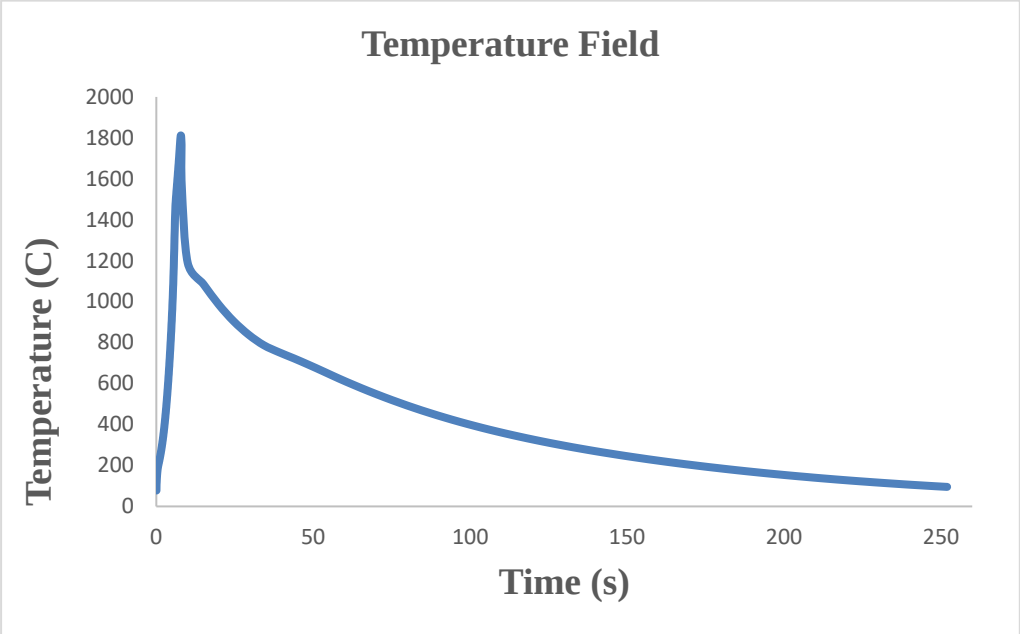

Figure 4-6: Temperature field generated

The temperature field generated during welding is the major reason due to which thermal stresses are induced. The maximum principal stress comes out to be positive on throat section which indicates it is tensile and the minimum principal stress is negative which indicates it is compressive. Also stress concentration is at the root of the weldment.

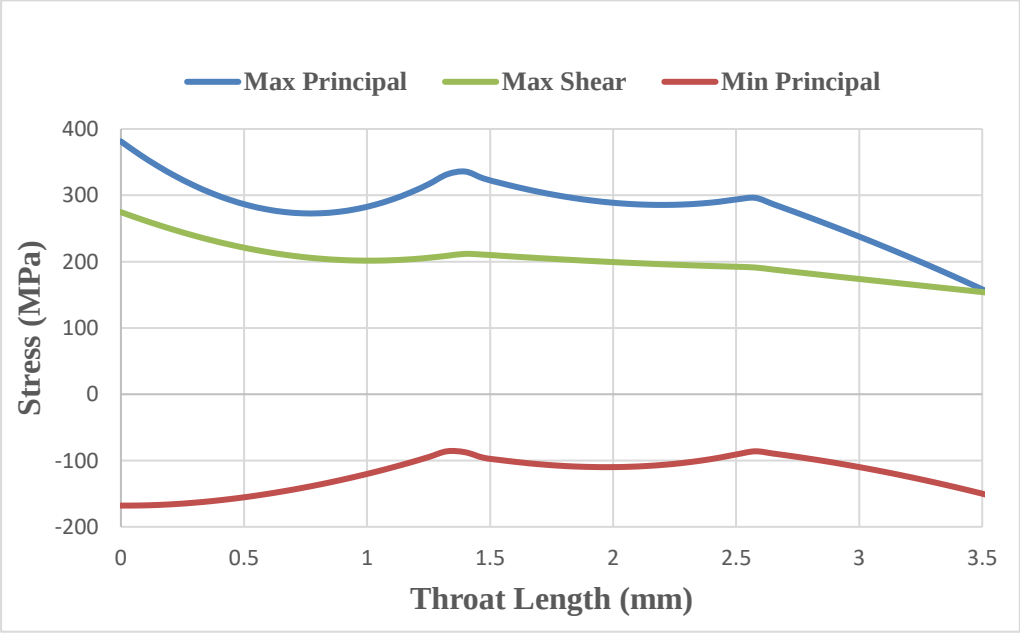

Figure 4-7: Stress distribution at the throat section in the presence of residual stresses

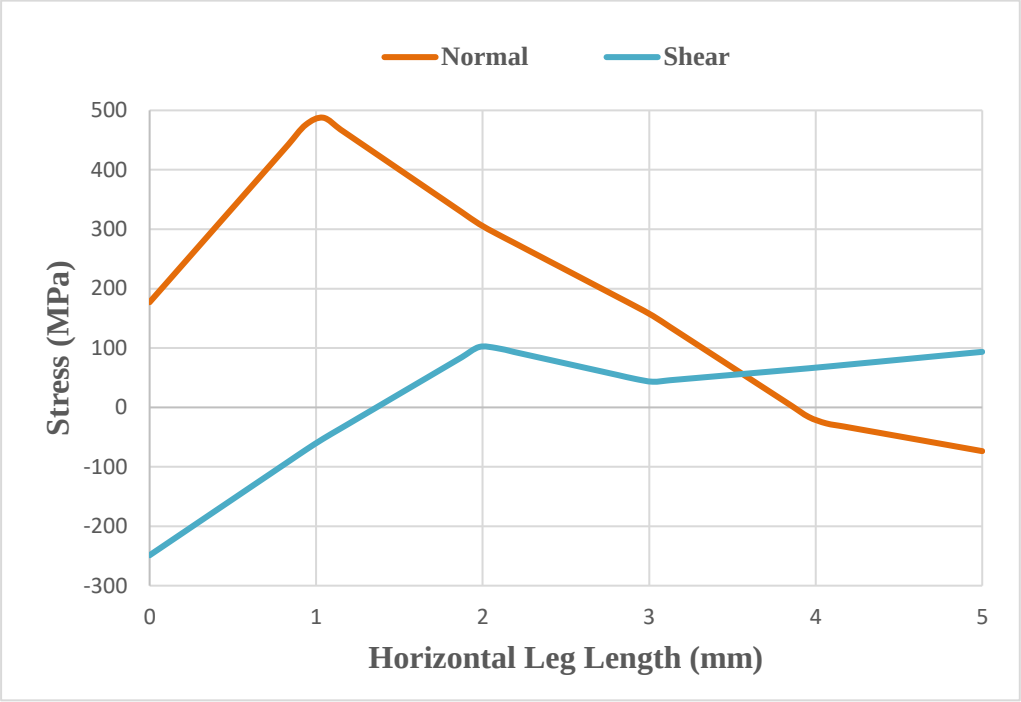

Figure 4-8: Stress distribution at the horizontal leg in the presence of residual stresses

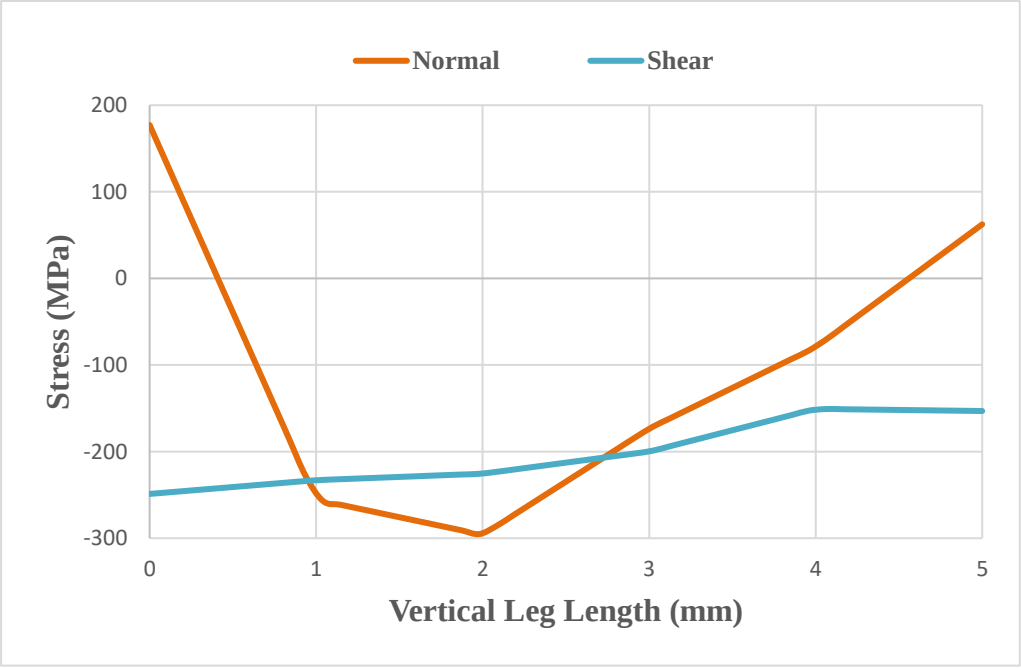

Figure 4-9: Stress distribution at the vertical leg in the presence of residual stresses

Comparison of stresses obtained in both cases are listed in table below;

	Without residual stresses (MPa)	**With residual stresses (MPa)**
Maximum Principal Stress Throat	1	381
Minimum Principal Stress Throat	7×10^{-5}	-86
Maximum Shear Stress Throat	0.8	274
Maximum Normal Stress Horizontal Leg	2.3	487
Maximum Shear Stress Horizontal Leg	-0.4	101
Maximum Normal Stress Vertical Leg	0.02	171
Maximum Shear Stress Vertical Leg	0.01	-151

CHAPTER 5: CONCLUSION

Stress distribution at the weldment of transverse fillet lap weld joint is validated at un-realistic set of boundary conditions. Effects of plate thickness and heat affected zone on the stress distribution are discussed. Stresses will approach to zero as we increase the plate thickness, or the heat affected zone. The elastic-plastic model is created using coupled field transient analysis. This model is an effective tool for exploring residual stresses that are generated during welding. Influence of residual stresses on stress distribution at the weldment is investigated using multilinear isotropic hardening plasticity model in coupled field transient analysis with non-linear steel A992 grade 50 material with realistic set of boundary conditions. Thermal and mechanical properties of steel A992 grade 50 at elevated temperature are used. Moving heat source is modelled using ACT extension in ANSYS workbench. Temperature field shows maximum temperature is at the weld region and decreases as it moves away from weld zone. Results show that due to the presence of residual stresses, the stress values at the weldment increased significantly and their behaviour is also very different. Stress concentration occurs at the root of the weldment.

5.1 RECOMENDATIONS

- In future, investigative analysis of the effect of material strength level on the prediction of residual stresses and distortions using continuous and intermittent fillet welds should be accurately studied.
- Also, numerical investigation and experimental investigation should be carried out with gap between plates to check the stress distribution on transverse fillet lap weld joint.

REFERENCES

1. Shigley, J., E., *Mechanical Engineering Design, Eleventh ed., McGraw-Hill Book Co.* New York, 2020. p. 486-524.

2. Norris, C., H., *Photoelastic investigation of stress distribution in transverse fillet welds*. Welding Journal, 1945. **24**: p. 557.

3. Salakian, A., G., and G. E. Claussen, *Stress distribution in fillet welds*: A Review of the Literature, Welding Journal, 1937. **16**: p. 1-24.

4. Hernandez, H., et al., *Improved scheme of analysis and stress computation in lap welded joints with fillet welds transversely and longitudinally loaded.* Conference Paper, 2005. p. 757-762.

5. Dawei, X., *An exact solution on the stress analysis of fillet welds*. Applied Mathematics and Mechanics, 1995. **16**(11): p. 1019-1024.

6. Vladulescu, F., et al., *Structural-thermal analysis of welded joints using ANSYS workbench platform*. Advanced Materials Research, 2018. **1146**: p. 17-21.

7. Barsoum, Z., and A. Lundback, *Simplified FE welding simulation of fillet welds - 3D effects on the formation of residual stresses*. Engineering Failure Analysis, 2009. **16**: p. 2281-2289.

8. Vemanaboina, H., et al., *Welding process simulation model for temperature and residual stress analysis*. Procedia Materials Science, 2014. **6**: p. 1539-1546.

9. Seif, M., et al., *Temperature dependent material modelling for structural steels*. Formulation and Application, 2016.

10. Eurocode 3. *Design of steel structures*. General rules. Structural fire design. Standard EN 1993-1-2, ECS (2005).

11. Deng, D., et al., *Determination of welding deformation in fillet welded joint by means of numerical simulation and comparison with experimental*

measurements. Journal of Materials Processing Technology, 2007. **183**: p. 219-225.

12. Miresmaeili, R., et al., *Experimental and numerical analyses of residual stress distributions in TIG welding process for 304L stainless steel*. Journal of Materials Processing Technology, 2008. **208**: p. 383–394.

13. Mollicone, P., et al., *Simple thermo-elastic-plastic models for welding distortion simulation.* Journal of Material Processing Technology, 2006. **176**: p. 77 – 86.

14. Deng, D., and H. Murakawa, *Prediction of welding distortion and residual stress in a thin plate butt-welded joint*. Computational Material Science, 2008. **3**: p. 353-365.

15. Chang, K., H., and C. H. Lee, *Finite element analysis of the residual stresses in T-joint fillet welds made of similar and dissimilar steels*. The International Journal of Advanced Manufacturing Technology, 2009. **41**: p. 250-258.

16. Brickstad, B., and B. L. Josefson, *A parametric study of residual stresses in multi-pass butt-welded stainless steel pipes*. International Journal of Pressure Vessels and Piping, 1998. **75**: p. 11-25.

17. Dike, J., J., et al., *Finite element modelling and validation of residual stresses in 304L girth welds*. In Trends in Welding Research, 5th International Conference, ASM International, Materials Park, Ohio, 1999. pp. 961-966.

18. Mollicone. P., et al., *Simple thermo-elastic-plastic models for welding distortion simulation*. Journal of Material Processing Technology, 2006. **176**: p. 77-86.

19. Perić, M., et al., *Numerical analysis and experimental investigation of welding residual stresses and distortions in a T-joint fillet weld*. Materials & Design, 2014. **53**: p. 1052-1063.

20. Qingyu, S., et al., *Development and application of the adaptive mesh technique in the three-dimensional numerical simulation of the welding process*. Journal of Materials Processing Technology, 2002. **121**: p. 167-172.

21. Kassab, R., et al., *Experimental and Finite Element Analysis of a T-Joint Welding*. Journal of Mechanics, 2012.

22. Seok, C., S., et al., *Investigation of welding residual stress of high tensile steel by finite element method and experiment.* KSME International Journal, 1999. **13**(12): p. 879-885.

23. Deng, D., et al., *Determination of welding deformation in fillet-welded joint by means of numerical simulation and comparison with experimental measurements*. Journal of Materials Processing Technology, 2007. **183**(2-3): p. 219-225.

24. Teng, T., L., et al., *Analysis of residual stresses and distortions in T-joint fillet welds*. International Journal of Pressure Vessels and Piping, 2001. **78**(8): p. 523-538.

25. Deng, D., et al., *Numerical and experimental investigations on welding residual stress in multi-pass butt-welded austenitic stainless-steel pipe*. Computational Materials Science, 2008. **42**: p. 234-244.

26. Ghafouri, M., et al., *Numerical and experimental investigations on the welding residual stresses and distortions of the short fillet welds in high strength steel plates*. Engineering Structures, 2022. **260**: p.114-269.

27. Deng, D., et al., *Investigating the influence of external restraint on welding distortion in thin-plate bead-on joint by means of numerical simulation and experiment*. The International Journal of Advanced Manufacturing Technology, 2016. **82**(5-8): p. 1049-1062.

28. Heinze, C., et al., *Numerical calculation of residual stress development of multi-pass gas metal arc welding*. Journal of Constructional Steel Research, 2012. **72**: p. 12-19.

29. Heinze, C., et al., *Numerical calculation of residual stress development of multi-pass gas metal arc welding under high restraint conditions.* Material & Design, 2012. **35**: p. 201-209.

30. Deng, D., et al., *Determining inherent deformations HSLA steel T-joint under structural constraint by means of thermal elastic plastic FEM*. Thin-Walled Structures, 2020. **147**: p. 106-568.

31. Rikken, M., et al., *A combined experimental and numerical examination of welding residual stresses*. Journal of Materials Processing Technology, 2018. **261**: p. 98-106.

32. Hemmesi, K., et al., *Numerical studies of welding residual stresses in tubular joints and experimental validations by means of x-ray and neutron diffraction analysis*. Materials & Design, 2017. **126**: p. 339-350.

33. Zhang, Y., and Y. Wang, *The influence of welding mechanical boundary condition on the residual stress and distortion of a stiffened panel*. Marine Structures, 2019. **65**: p. 259-270.

34. Lourenco, M., I., et al., *Effect of boundary conditions on residual stress and distortion in T-joint welds*. Journal of Constructional Steel Research, 2014. **102**: p. 121-135.

35. Shen, J., and Z. Chen, *Welding simulation of fillet-welded joint using shell elements with section integration*. Journal of Materials Processing Technology, 2014. **214**: p. 2529-2536.

36. Seles, K., et al., *Numerical simulation of a welding process using a prescribed temperature approach*. Journal of Constructional Steel Research, 2018. **145**: p. 49-57.

37. Bhatti, A., A., et al., *Influence of thermo-mechanical material properties of different steel grades on welding residual stresses and angular distortion*. Materials & Design, 2015. **65**: p. 878-889.

38. Ahola, A., et al., *On the design of fillet welds made of ultra-high strength steel*. Welding in the World, 2018. **62**: p. 985-995.

39. Wu, A., *Finite element modelling for the assessment of residual stresses and failure mechanisms in welded connections*. Materials Research Group, 2004.

40. Sarkani, S., et al., *An efficient approach for computing residual stresses in welded joints*. Finite Element in Analysis and Design, 2000. **35**(3): p. 247-268.

41. Cai, W., et al., *True stress-strain curves for ASTM A992 steel for fracture simulation at elevated temperatures*. Journal of Constructional Steel Research, 2018. **194**.